

9-1-2007

# Computation of Electromagnetic Fields in Assemblages of Biological Cells Using a Modified Finite-Difference Time-Domain Scheme


C H. See

R.A. Abd-Alhameed

Peter S. Excell

*Glyndwr University*, p.excell@glyndwr.ac.uk

Follow this and additional works at: <http://epubs.glyndwr.ac.uk/cair>

 Part of the [Biomedical Commons](#), and the [Computational Engineering Commons](#)

## Recommended Citation

See, C. H., Abd-Alhameed, R. A. & Excell, P. S. (2007) 'Computation of Electromagnetic Fields in Assemblages of Biological Cells Using a Modified Finite-Difference Time-Domain Scheme'. *IEEE Transactions on Microwave Theory and Techniques*, 55(9), 1986-1994.

This Article is brought to you for free and open access by the Computer Science at Glyndŵr University Research Online. It has been accepted for inclusion in Computing by an authorized administrator of Glyndŵr University Research Online. For more information, please contact [d.jepson@glyndwr.ac.uk](mailto:d.jepson@glyndwr.ac.uk).

---

# Computation of Electromagnetic Fields in Assemblages of Biological Cells Using a Modified Finite-Difference Time-Domain Scheme

## Abstract

When modeling objects that are small compared with the wavelength, e.g., biological cells at radio frequencies, the standard finite-difference time-domain (FDTD) method requires extremely small time-step sizes, which may lead to excessive computation times. The problem can be overcome by implementing a quasi-static approximate version of FDTD based on transferring the working frequency to a higher frequency and scaling back to the frequency of interest after the field has been computed. An approach to modeling and analysis of biological cells, incorporating a generic lumped-element membrane model, is presented here. Since the external medium of the biological cell is lossy material, a modified Berenger absorbing boundary condition is used to truncate the computation grid. Linear assemblages of cells are investigated and then Floquet periodic boundary conditions are imposed to imitate the effect of periodic replication of the assemblages. Thus, the analysis of a large structure of cells is made more computationally efficient than the modeling of the entire structure. The total fields of the simulated structures are shown to give reasonable and stable results at 900, 1800, and 2450 MHz. This method will facilitate deeper investigation of the phenomena in the interaction between electromagnetic fields and biological systems.

## Keywords

generic lumped-element membrane, quasi-static, floquet periodic, electromagnetic fields, biological systems, microdosimetric modeling, bioelectromagnetic interactions, verisimilitude, electromagnetic fields, assemblages

## Disciplines

Biomedical | Computational Engineering | Electrical and Computer Engineering

## Comments

©2007 IEEE. Personal use of this material is permitted. However, permission to reprint/republish this material for advertising or promotional purposes or for creating new collective works for resale or redistribution to servers or lists, or to reuse any copyrighted component of this work in other works must be obtained from the IEEE. This material is presented to ensure timely dissemination of scholarly and technical work. Copyright and all rights therein are retained by authors or by other copyright holders. All persons copying this information are expected to adhere to the terms and constraints invoked by each author's copyright. In most cases, these works may not be reposted without the explicit permission of the copyright holder. The paper was published by IEEE Transactions on Microwave Theory and Techniques in 2007 and the definitive version is available at [www.ieeexplore.ieee.org](http://www.ieeexplore.ieee.org)

# COMPUTATION OF ELECTROMAGNETIC FIELDS IN ASSEMBLAGES OF BIOLOGICAL CELLS USING A MODIFIED FDTD SCHEME

C.H. See, R.A. Abd-Alhameed and P.S. Excell  
Mobile and Satellite Communications Research Centre,  
Bradford University, Bradford, UK  
Email: c.h.see1@bradford.ac.uk, r.a.a.abd@bradford.ac.uk, p.s.excell@bradford.ac.uk

## ***ABSTRACT:***

When modeling scattering objects that are small compared with the wavelength, the standard Finite-Difference Time-domain (FDTD) method requires extremely small time-step sizes. This is especially so in modeling biological cells having sizes of the order of a few tens of micrometers. This can become impractical due to the very large computation times required. This problem can be overcome by implementing a quasi-static approximate version of FDTD, based on transferring the working frequency to a higher frequency, to reduce the number of time steps required. Then, the generated internal field at the higher frequency can be scaled back to the frequency of interest. This paper presents an approach to modeling and analysis of the Hodgkin and Huxley (HH) membrane model, represented as an electrical circuit on the surface of a biologically equivalent spherical and cubical cell: the cubical shape being investigated to facilitate packing. Since the external medium of the biological cell is lossy material, a modified Berenger perfectly matched layer absorbing boundary condition is used to truncate the computation grid, in order to reduce the reflections on the interface layers. Linear assemblages of such cells are investigated and then Floquet periodic boundary conditions are imposed over the border of the simulated structures to imitate the effect of periodic replication of the remaining cells. Thus, the analysis of a large structure of cells is made much simpler and more computationally efficient than the modeling of the entire structure. The total fields of the simulated structures have been shown to give reasonable and stable results at 900MHz, 1800MHz and 2450MHz.

This tool will facilitate deeper investigation of the phenomena in the interaction between EM fields and biological systems at various levels of spatial definition.

*Key words:* Finite-Difference Time Domain (FDTD); quasi-static method; HH (Hodgkin and Huxley) membrane model; Floquet Periodic Boundary Conditions.

## 1. INTRODUCTION

Research into possible mechanisms of interaction of electromagnetic (EM) fields with biological tissues and cells in culture has motivated a growing need for accurate models describing the EM behavior of cells exposed to these fields. Therefore, several numerical models have been created in order to study the interaction between EM fields and biological entities, at tissue level, cell level and ionic level. In this area, the most frequently used technique for computing the EM field is the finite-difference time-domain (FDTD) method [1,2], due to its independence from the material parameters.

The original Finite-Difference Time-Domain (FDTD) method requires extremely small time-step sizes when modeling electrically-small regions (much smaller than a wavelength): this is especially the case when modeling biological cells, since they have maximum dimensions of a few tens of micrometers. Thus, it can become impractical due to the unaffordable computation times required. This problem can be solved by implementing a quasi-static approximate version of FDTD. This approach is based on transferring the working frequency to a higher frequency, to reduce the number of time steps required. Then, the generated internal field at the higher frequency can be scaled back to the frequency of interest [3-6].

Cells are surrounded by thin membranes, typically a few nanometres thick [7]. They are the major barrier in the cell, separating the inside of the cell from the exterior medium. It is this structure which allows cells to selectively interact with their environment. Therefore, the cell membrane has been identified as the primary target for the study of possible actions of EM fields on biological structures. Since the thickness of the membrane is about 1000 times smaller than the biological cell, if the standard FDTD procedure were to be blindly applied to model detail in the membrane within a complete cell model, this would cause some millions of iterations to be required to complete one cycle of simulation. This again will cause excessive computation time. To overcome this drawback in standard FDTD, the lumped element finite different time domain (LE-FDTD) method [8-11] was implemented to model the behavior of the membrane, based on the Hodgkin-Huxley (HH) model [12-16] on the surface of the biological cell.

This paper presents the new approach to modeling and analysis of the HH (Hodgkin and Huxley) membrane model which is represented as an electrical circuit on the surface of the biological equivalent spherical cells. For the sake of simplicity, the analyzed structure has been represented with spherical or cubical cells and Floquet periodic boundary conditions [17-20] have been applied to the border of the analyzed structure in order to mimic the presence of the surrounding cells. Although cellular tissues are not perfectly periodic and living cells are not precisely spheres or cubes, this approximation allows a reasonable approximation to the modeling of biological tissue using only a small part of the structure, while alleviating the problem of the huge requirement of computer resources for the simulation of a complete body of tissue. Since the external medium of the biological tissue is lossy fluid, the modified Berenger perfectly matched layer (PML) absorbing boundary condition (ABC) [21-24] is used to truncate the computation grid, in order to reduce the reflections on the interface layers: this is more accurate than the Mur ABC [25, 26], used in other recent work [4].

A further difficulty is the limited extent of studies on the dielectric properties of cell tissues [27]; thus, the complex permittivity of each cell tissue is not clearly established for radio frequencies. However, in this study, an analytical method for estimating the electrical properties of cell tissues in the RF band [28], will be adopted throughout the analysis. Earlier work only considered two media (water and membrane) [4], but the procedure adopted here enables the tissue model to consist of three media (lossy medium, membrane and cytoplasm). In addition, a mass of connected biological tissue is simulated by creating an equivalent stack of compacted cells (both spherical, with interstices, and fully-compacted cubical). The total electric fields along the central axes of rows of these spherical and cubical cellular structures will be investigated.

## **2. SUMMARY OF METHOD**

### **2.1 Quasi-Static FDTD Scheme**

The interaction between animals and humans exposed to extremely low frequency electric fields was investigated by Kaune and Gillis [29] and Guy et al. [30] in 1981 and 1982 respectively. Their research outcomes furnish valuable analytical and experimental verification of the concept of quasi-static coupling at power-line frequencies. Later authors [5,6,31] implemented the same principles using finite difference time domain (FDTD) to study the numerical dosimetry of anatomically-based models.

Recently, the same idea was further extended to modeling the interaction between electromagnetic (EM) fields and biological tissue at mobile communication frequencies, i.e. GSM900 and GSM1800 [4].

In order to implement the quasi-static approximation to analyze scattering problems, the following two conditions have to be satisfied [29, 30]:

$$1. d_{\max} < \lambda/10 \quad (1a)$$

$$2. |\sigma + j\omega\epsilon| \gg \omega\epsilon_0 \quad (1b)$$

where  $d_{\max}$  is the maximum dimension of the structure under investigation,  $\lambda$  is the wavelength, and  $\sigma$  and  $\epsilon$  are the conductivity and permittivity of the analyzed structure respectively,  $\omega$  is the radian frequency, and  $\epsilon_0$  is the permittivity of free space.

Under these conditions, electric fields outside the analyzed object do not depend significantly on the internal object properties, but only on the shape of the body, the components of the electric field tangential to the surface of the model and the internal fields being approximately zero compared to the applied field. For these conditions, the external field  $E$  at the object's surface can be considered to be perpendicular to its surface.

From the Maxwell equation  $\text{div } \mathbf{D} = \rho$ , the boundary condition for the normal component of electric field at the surface of the region of interest is :

$$j\omega\epsilon_0 \hat{n} \cdot \vec{E}_{air} = (\sigma_{tissue} + j\omega\epsilon_{tissue}) \hat{n} \cdot \vec{E}_{tissue} \quad (2)$$

From equation (2), under the two conditions given in (1a,b), a scaling relationship between the fields at frequencies  $f$  and  $f'$  can be derived as follows [5,30]:

$$\vec{E}_{tissue}(f) = \left( \frac{\omega}{\omega'} \right) \left[ \frac{\sigma'(f') + j\omega'\epsilon(f')}{\sigma(f) + j\omega\epsilon(f)} \right] \vec{E}'_{tissue}(f')$$

$$\cong \left[ \frac{f\sigma'(f')}{f'\sigma(f)} \right] \bar{E}'_{tissue}(f') \quad (3)$$

Assuming that  $\omega\epsilon(f) \ll \sigma(f)$  and  $\omega'\epsilon'(f') \ll \sigma'(f')$ , then according to equation (3), a higher working frequency ( $f'$ ) which still falls within the quasi-static regime, can be chosen to excite the model, to reduce the computation time. Thus, the resultant internal fields,  $E'$ , evaluated at that frequency can be transferred back to the desired low frequency with negligible error. Since the induced current densities and internal electric fields are proportional to the frequency, the magnetic fields hold a similar scaling relationship.

## 2.2 Modified Berenger PML

The Perfectly Matched Layer (PML), introduced by Berenger [21] in 1994, allowed boundary reflections below -80dB to be realised. PML is based on surrounding the FDTD problem space with a highly lossy and matched non-physical absorber. It has been found to be the most accurate technique of the ABCs available and has become standard in most current FDTD implementations [32]. For the case of PML layers with conductivities increasing geometrically, the geometric grading factor ( $g$ ) can be modified in order to reduce the reflection on the interface layer when the problem space is entirely within a lossy-medium environment. An empirical expression from which  $g$  can be found, and which has been found to give good results [23, 24] is:

$$\sigma = -\frac{\epsilon c}{2\Delta x} \frac{\ln g}{g^N - 1} \ln R(0) \quad (4)$$

where  $\Delta x$  is the spatial increment of the FDTD mesh,  $R(0)$  is the normal reflection coefficient,  $N$  is the number of the cells in the PML thickness,  $c$  is the velocity of EM waves in the environment concerned.



### **2.3 Floquet Periodic Boundary Condition (PBC)**

Many structures of electromagnetic interest are electrically very large and hence pose great difficulties for computational simulation. One approach that can be used to reduce the size of the computational task is to exploit any periodicity in the structure, in one and more dimensions: this concept will be exploited here, assuming that a sample of tissue is formed from a periodic grid of biological cells. In order to perform EM analysis on these types of structure with reasonable computational time, the structures are assumed to be an infinite grid and the problem can then be reduced to a unit-cell analysis via use of the Floquet boundary condition to simulate the effect of the periodic replication.

The finite-difference time-domain (FDTD) technique was applied to the basic structure due to its simplicity and flexibility. FDTD has already been successfully extended to incorporate the Floquet theorem for the case of normal [17, 33] and oblique incidence [34, 35] for two- and three-dimensional problems. The techniques used to combine FDTD with the Floquet periodic boundary condition can be classified into two categories, i.e., direct field methods and field transformation methods. Direct field methods include Normal incidence, Sine-Cosine, Multiple Unit Cell and Angled Update Methods, while field transformation methods include Multi-Spatial Grid and Split-Field methods [2].

### **2.4 HH (Hodgkin and Huxley) Membrane Model**

Cells are surrounded by a thin membrane, which is the major barrier, separating the cell from its (normally) fluid environment. Since the cell needs to get nutrients in and waste out, the membrane must be able to accommodate this. Therefore, the membrane has to act as a selective barrier, allowing nutrients to pass in but keeping out many substances harmful to the cell, and acting as a dynamic barrier medium, constantly adapting to changing environmental conditions (e.g. different concentrations of ions).

The dimensions of a biological cell are around a few tens of micrometers and the thicknesses of the membranes are in the scale of a few nanometers, strongly depending on the type of the tissue. Depending on the type of the cell, voltages in the range of 20-200mV can arise across the membrane. When the cell is in a resting state, the current across the membrane averages zero, but more generally it

depends on the variation of the membrane voltage [12].

Hodgkin and Huxley (HH) gave a general description of the time course of the current which flows through the membrane of the squid giant axon when the potential difference across the membrane was suddenly changed from its steady state. The results in [12] suggest that the behaviour of membrane may be represented by the electrical circuit shown in Fig. 1. Current can be carried through the membrane either by charging the membrane capacitance or by movement of ions through the nonlinear conductance in parallel with the membrane capacitance. A set of equations governing the model is given in [4, 12].

### **3. IMPLEMENTATION AND VALIDATION**

#### **3.1 HH model implementation**

To verify the correctness of the implementation of the HH model within the FDTD framework, the results of the analytically computed solution have been used for comparison. The HH model was implemented on a spherical structure with diameter 50  $\mu\text{m}$  and discretised with 1  $\mu\text{m}$  steps, in order to check for the expected polarization voltage of 60.27 mV on the membrane [\*Ref\*]. The HH model is included on the surface of the cell, while the regions internal and external to the sphere were considered as cytoplasm and lossy medium respectively. It should be noted that the LE-FDTD method has been successfully modified in order to allow arbitrary positioning of the lumped element inside the membrane's cell, not necessarily aligned with the FDTD grid (see Fig.2), so that it represents the structure more exactly than simple FDTD. Fig. 3 depicts the expected polarization voltage of 60.27mV, appearing on the membrane of the spherical structure without any external excitation.

### 3.2 Quasi-static FDTD validation

In this section, a simple example will be given to illustrate this method: the obtained results will be compared with the Mie series analytical solution [36, 37]. A two-layer sphere simulating a biological cell inside a lossy medium was considered, for which the assumed properties were as follows: cytoplasm (internal)  $\epsilon_r = 48.699$ ,  $\sigma = 1.412$ ; membrane  $\epsilon_r = 11.3$ ,  $\sigma = 0.0$ ; and lossy medium (external)  $\epsilon_r = 70.87$ ,  $\sigma = 2.781$ . The internal radius (internal region) was  $25\mu\text{m}$  and the membrane thickness was set to  $2\mu\text{m}$ . The operating frequency was 2.45 GHz, whereas the interim transformed frequency used in this example was 30 GHz. From equation (4), the optimum grading factor  $g$  is 6.07 for an FDTD cell size of  $1\mu\text{m}$ . It should be noted that this model in the FDTD computation domain is excited by a standard plane wave of amplitude 1V/m, propagating in the  $z$ -direction and polarized in the  $x$ -direction. The field distributions along the two central axes of the layered cell are depicted in Fig.4 and Fig.5. As can be clearly seen, the numerical results are in good agreement with the analytical ones.

## 4. SIMULATION AND RESULTS

### 4.1 Connected Tissue Model Using Spherical Cells

A stack of ten spherical cells was investigated, as shown in Fig.6 and Fig.7. The radius of the each cell was  $10\mu\text{m}$ . The model contains three media, cytoplasm, membrane and extracellular medium and the dielectric properties of these were obtained from [28], as tabulated in Table 1. A plane wave of 100 V/m, propagating in the  $z$ -direction and polarized in the  $x$ -direction was used as the excitation. Note that the incident plane wave excitation is applied on a plane lying between the PML region and the outer limit of the FDTD grid. In addition, in order to reduce high-frequency transients [38, 39] and DC offsets [40, 41] sometimes associated with unramped sine wave excitations, the ramped sinusoidal source in equation (4) was adopted. In general, this can be done by multiplying the excitation source of 100Vm with the  $f(t)$  functions given, varying for different ranges of  $t$ , as shown in equation (5) [40].

$$f(t) = \begin{cases} 0 & t < 0 \\ 0.5[1 - \cos(\omega_r t)]\sin(\omega_r t) & 0 \leq t \leq \frac{T_r}{2} \\ \sin(\omega_r t) & t > \frac{T_r}{2} \end{cases} \quad (5)$$

Where  $T_r$  is the duration of the ramped cosine regime, which is about 3 source cycles.

Fig.6 and Fig.7 illustrate the 2-D and 3-D view of the basic configuration of the structure analyzed. As shown in Fig.7, the PML was 6 FDTD cells wide, the grading factor for optimal ABC was 7.957 and the grid structure was effectively extended to infinity in the x- and y-directions, by imposing the Floquet boundary condition along the x and y axes. The Floquet periodic boundary condition (PBC) plays an important role to mimic the presence of an extended 3-dimensional structure of biological cells, simulating connected tissue. This can be easily imagined in two dimensions, as shown in Fig.6. The FDTD problem space was 220 x 20 x 20 FDTD cells of size 1 $\mu$ m while a discretization time step  $\delta t$  of 1.3 femtosecond was chosen to drive the FDTD computation to meet the requirements of the Courant stability criterion.

Before implementing the HH model into the simulated structure, the effect of moving the Floquet PBCs gradually away from the simulated structure was studied. Fig. 8 and Fig.9 depict the field distribution through the centre of the simulated structure at 10GHz with varying locations of the PBC, where Ncell is the number of FDTD cells between the Floquet PBCs and the boundaries of the *biological* cells, in the x and y directions. Fig. 10 shows the field distribution on the xz-plane of the simulated structure for the case of Ncell = 10. When the PBCs are exactly adjacent to the simulated structure (Ncell = 0), the strongest coupling effect between cells can be obtained: the highest induced field on the membrane and lowest induced field in the cytoplasm of the cell can be observed. Conversely, when the PBCs are far away from the simulated structure (Ncell = 10), the lowest induced field on the membrane and highest induced field in the cytoplasm of the cell are observed. It should be noted that all the following analysis will be based on Ncell = 0, which is assumed to be the most appropriate model for the real living biological tissues or cells in this micro-dosimetry study.

The simulations are performed at the transformed intermediate frequency of 10GHz and the overall model is then transformed to the intended lower frequencies: Table 2 reports the transformation factors at 900MHz, 1800MHz, 2000MHz and 2450MHz that were used in the analysis. These can be calculated by substituting the parameters from Table 1 into equation (3).

Fig.11 illustrates the 10GHz field distribution on the xz-plane of the simulated structure. The distributions of the electric field through the centre of the simulated structure, along the incident wave propagation direction, at 900MHz, 1800MHz, 2000MHz and 2450MHz are given in Fig.12 and Fig.13, where Fig.13 is an enlarged version of Fig.12. From inspection of Fig.13, the field inside the cells is not constant and the induced field intensity is directly proportional to the frequency. In the other words, the higher the operating frequency that is used to excite the model, the higher the electric field intensity that will be induced within the analyzed structures.

To complete the simulation, the HH models are embedded in the surface of the spherical cells, in a direction normal to the surface, to represent the membrane effect of the tissue model. Versions including this were studied at frequencies of 900MHz and 2450MHz. As can be seen in Fig. 14 and Fig.15, there is an explicit difference of approximately 15% in the field strength due to the contribution of the membrane effect from the HH model. In general, these variations were in well agreement with expectations [4, 12, 28].

(\*\*How was the HH model scaled in frequency?? This question was asked in Rome as well)

## 4.2 Cubical Cells Model

Since living cells, when compacted into connected tissue, are not perfect spheres, a cluster of cubical cells was chosen for study on the foundation of the previous spherical-cells analysis. Fig.16 depicts the proposed cluster of cubical cells in a three dimensional view of the FDTD computational domain. In order to compare the results obtained from the previous model to this analysis, the FDTD simulation was executed, keeping the same FDTD parameter values as in the previous configuration. The 2D view of the electric field inside the cubical-cell tissue is shown in Fig. 17. The field distributions along the propagation direction of the incident wave, through the centre of the simulated structure at various

frequencies are illustrated in Fig.18 and Fig.19. Moreover, the contribution of the HH model to the cubical tissue model has also been investigated, as shown in Fig.20 and Fig.21. The effect of adding the HH model is about 15% difference in field, as can be seen from the figure.

The peak field on the membrane of the cubical structure is observed to be about three times higher than in the cytoplasm which agrees well with the results from the structure based on spherical cells. However, the absolute field strength is approximately doubled in the spherical-cell case, presumably because of the curvature at the point studied: it is to be expected that much higher fields would be observed at the corners of the cubical cells, but it might be argued that, as a localised matter, these points do not correspond well with biological reality.

## **5. CONCLUSION**

An approach to microdosimetric modeling of bioelectromagnetic interactions at the cellular level has been presented. This uses the FDTD method, combined with an arbitrarily-oriented implementation of the Hodgkin-Huxley cell-membrane model and the Floquet periodic boundary condition. By implementing a frequency-scaling approach, the number of FDTD time steps for such an electrically-small structure can be reduced from several millions to a few tens of thousands. The reflection on the interface layers inside the FDTD computation domain has also been successfully reduced, even though it is within lossy penetrable media, by using a modified version of Berenger's PML absorbing boundary condition. The accuracy of the FDTD scaling approach was verified with idealized models of spherical cells in lossy media. The feasibility of the inclusion of the HH model inside the FDTD computation domain was demonstrated. This leads to the conclusion that the application of the HH model allows cells of arbitrary geometries to be handled and demonstrates the viability of embedding other types of lumped-element model for membrane behavior.

Use of the Floquet boundary condition enables a non-trivial region of connected biological tissue to be simulated. Such a tool will facilitate deeper investigation of the phenomena in the interaction between EM fields and biological systems at various levels of spatial definition. The combination of quasi-static FDTD with an arbitrarily-oriented lumped element membrane model, the modified Berenger

ABC and the Floquet periodic boundary condition represents a significant advance in verisimilitude of biological cell modeling.

(\* 'Numerical Noise' sentence deleted – you can't introduce a new issue in the Conclusions! Either discuss it in the main text or forget it)

## REFERENCES

- [1] K. S. Yee, "Numerical solution of initial boundary value problems involving Maxwell's equation in isotropic media," *IEEE Trans. on Antennas Propagation*, vol. AP-14, pp. 302-307, 1966.
- [2] A. Taflove and S. C. Hagness, *Computational Electrodynamics: The Finite-Difference Time-Domain*, 2nd ed: Artech House:Boston, 2000.
- [3] O. P. Gandhi, "FDTD in Bioelectromagnetics: Safety Assessment and Medical Applications," in *Advances in Computational Electrodynamics: The Finite-Difference Time-Domain Method*, A. Taflove, Ed., 1st ed: Artech House, 1998, pp. 627-632.
- [4] G. Emili, A. Schiavoni, F. L. Roselli, and R. Sorrentino, "Computation of electromagnetic field inside a tissue at mobile communications frequencies," *IEEE Trans on MTT*, vol. 51, pp. 178-186, 2003.
- [5] O. P. Gandhi and J. Chen, "Numerical dosimetry at power-line frequencies using anatomically based models," *Bioelectromagnetics*, vol. 1, pp. 43-60, 1992.
- [6] M. E. Potter, M. Okoniewski, and M. A. Stuchly, "Low Frequency Finite Difference Time Domain (FDTD) for Modelling of Induced Fields in Humans Close to Line Sources," *Journal of computational physics*, vol. 162, pp. 82-103, 2000.
- [7] L. M. Liu and S. F. Cleary, "Absorbed Energy distribution from radio frequency electromagnetic radiation in a mammalian cell model: Effect of membrane-Bound water," *Bioelectromagnetics*, vol. 16, pp. 160-171, 1995.
- [8] W. Sui, D. A. Christensen, and C. H. Durney, "Extending the two-dimensional FDTD method to hybrid electromagnetic systems with active and passive lumped elements," *IEEE Trans. MTT*, vol. MTT-40, pp. 724-730, 1992.
- [9] M. Picket-May, A. Taflove, and J. Baron, "FDTD modeling of Digital Signal Propagation in 3D circuits with Passive and Active Loads," *IEEE Trans. MTT*, vol. MTT-42, pp. 1514-1523, 1994.
- [10] P. Ciampolini, P. Mezzanotte, L. Roselli, D. Sereni, P. Torti, and R. Sorrentino, "Simulation of HF circuits with FDTD technique including nonideal lumped elements," in *IEEE MTT-S Int. Microwave Symp. Digest. Orlando FL*, pp. 361-364, 1995.
- [11] C. N. Kuo, B. Houshmand, and T. Itoh, "Full-Wave Analysis of Packaged Microwave Circuits with Active and Nonlinear Devices: An FDTD Approach," *IEEE Transactions on Microwave Theory and Techniques*, vol. 45, pp. 819-826, 1997.
- [12] A. L. Hodgkin and A. F. Huxley, "A quantitative description of membrane current and its application to conduction and excitation in nerve," *J. Physiol.*, vol. 117, pp. 500-544, 1952.
- [13] A. L. Hodgkin and A. F. Huxley, "Current carried by sodium and potassium ions through the membrane of the giant axon of Loligo," *J. Physiol.*, vol. 116, pp. 449-472, 1952.

- [14] A. L. Hodgkin, A. F. Huxley, and B. Katz, "Measurement of current-voltage relations in the membrane of the giant axon of Loligo," *J. Physiol.*, vol. 116, pp. 424-448, 1952.
- [15] A. L. Hodgkin and A. F. Huxley, "The components of membrane conductance in the giant axon of Loligo," *J. Physiol.*, vol. 116, pp. 473-496, 1952.
- [16] A. L. Hodgkin and A. F. Huxley, "The dual effect of membrane potential on sodium conductance in the giant axon of Loligo," *J. Physiol.*, vol. 116, pp. 497-506, 1952.
- [17] W. J. Tsay and D. M. Pozar, "Application of the FDTD Technique to Periodic Problems in Scattering and Radiation," *IEEE Microwave and Guided Wave Letters*, vol. 3, pp. 250-252, 1993.
- [18] J. Ren, O. P. Gandhi, L. R. Walker, J. Fraschilla, and C. R. Boerman, "Floquet-Based FDTD Analysis of Two-dimensional Phased Array Antennas," *IEEE Microwave and Guided Wave Letters*, vol. 4, pp. 109-111, 1994.
- [19] A. Alexanian, N. J. Koliass, R. C. Compton, and R. A. York, "Three-dimensional FDTD analysis of quasi-optical arrays using Floquet boundary conditions and Berenger's PML," *IEEE Microwave and Guided Wave Letters*, vol. 6, pp. 138-140, 1996.
- [20] J. G. Maloney and M. P. Kesler, "Analysis of Periodic Structures," in *Computational Electrodynamics: The Finite-Difference Time-Domain Method*, A. Taflov, Ed., 2nd ed. London: Artech House, 2000, pp. 569-625.
- [21] J. Berenger, "A perfectly matched layer for Absorption of Electromagnetic waves," *Journal of computational physics*, vol. 114, pp. 185-200, 1994.
- [22] D. S. Katz, E. T. Thiele, and A. Taflove, "Validation and Extension to Three Dimensions of the Berenger PML Absorbing Boundary Condition for FD-TD Meshes," *IEEE Trans. on Microwave and Guided Wave Letters*, vol. 4, pp. 268-270, 1994.
- [23] J. Berenger, "Perfectly Matched layer for the FDTD Solution of wave-structure interaction problems," *IEEE Trans. on Antennas and Propagation*, vol. 44, pp. 110-117, 1996.
- [24] J. Berenger, "Improved PML for the FDTD solution of wave-structure Interaction problem," *IEEE Trans. on Antennas and Propagation*, vol. 45, pp. 466-473, 1997.
- [25] *International FDTD database: URL: <http://www.fDTD.org>.*
- [26] G. Mur, "Absorbing boundary conditions for the Finite-Difference Approximation of the time-domain Electromagnetic-field equations," *IEEE Trans. on Electromagnetic compatibility*, vol. EMC-23, pp. 377-382, 1981.
- [27] H. Ebara, K. Tani, T. Onishi, S. Uebayashi, and O. Hashimoto, "Method for Estimating Complex Permittivity Based on Measuring Effective Permittivity of Dielectric Mixtures in Radio Frequency Band," *IEICE Trans. Commun.*, vol. E88-B, pp. 3269-3274, 2005.
- [28] T. Kotnik and D. Miklavcic, "Theoretical Evaluation of the Distributed Power Dissipation in Biological cells Exposed to Electric Fields," *Bioelectromagnetics*, vol. 21, pp. 385-394, 2000.
- [29] W. T. Kaune and M. F. Gillis, "General Properties of the Interaction Between Animals and ELF Electric Fields," *Bioelectromagnetics*, vol. 2, pp. 1-11, 1981.
- [30] A. W. Guy, S. Davidow, G. Y. Yang, and C. K. Chou, "Determination of Electric Current Distributions in Animals and Humans Exposed to a Uniform 60-Hz High-Intensity Electric Field," *Bioelectromagnetics*, vol. 3, pp. 47-71, 1982.
- [31] J. D. Moerlose, T. W. Dawson, and M. A. Stuchly, "Application of the finite difference time domain algorithm to quasi-static field analysis," *Radio Science*, vol. 32, pp. 329-341, 1997.
- [32] D. T. Prescott and N. V. Shuley, "Reflection Analysis of FDTD Boundary Conditions -Part II: Berenger's PML Absorbing Layers," *IEEE Trans on MTT*, vol. 45, pp. 1171-1178, 1997.



- [33] E. A. Navarro, B. Gimeno, and J. L. Cruz, "Modelling of periodic structures using the finite-difference time-domain method combined with the floquet theorem," *Electronic Letters*, vol. 29, pp. 446-447, 1993.
- [34] M. E. Veysoglu, R. T. Shin, and J. A. Kong, "A finite-difference time-domain analysis of wave scattering from periodic surfaces: Oblique incidence case," *J. Electron. Waves Appl.*, vol. 7, pp. 1595-1607, 1993.
- [35] D. T. Prescott and N. V. Shuley, "Extensions to the FDTD Method for the Analysis of Infinitely Periodic Arrays," *IEEE Microwave and Guided Wave Letters*, vol. 4, pp. 352-354, 1994.
- [36] G. Mie, "contributions to the optics of diffusing media," *Ann. Physik*, vol. 25, pp. 377, 1908.
- [37] J. R. Mautz, "Mie Series Solution for a Sphere," *IEEE Trans. on MTT*, vol. 26, pp. 375, 1978.
- [38] C. M. Furse, J. Y. Chen, and O. P. Gandhi, "The use of the frequency-dependent finite-difference time-domain method for induced current and SAR calculations for a heterogeneous model of the human body," *IEEE Transactions on Electromagnetic Compatibility*, vol. 36, pp. 128-133, 1994.
- [39] D. H. Roper and J. M. Baird, "Analysis of Overmoded Waveguides Using the Finite-Difference Time Domain Method," *IEEE MTT-S International Microwave Symposium Digest*, pp. 401-404, 1992.
- [40] C. M. Furse, S. P. Mathur, and O. P. Gandhi, "Improvements to the finite-difference time-domain method for calculating the radar cross section of a perfectly conducting target," *IEEE Transactions on Microwave Theory and Techniques*, vol. 38, pp. 919-927, 1990.
- [41] C. M. Furse, D. H. Roper, D. N. Buechler, D. A. Christensen, and C. H. Durney, "The Problem of Treatment of DC offsets in FDTD Simulations," *IEEE Transactions on Antennas and Propagations*, vol. 48, pp. 1198-1201, 2000.

***List of Figures and Tables:***

Table 1. Electrical properties of the simulated media at relevant frequencies

Table 2. Frequency scaling transformation factor from 10GHz to the mobile communication frequencies given

Fig.1: Equivalent electrical circuit for the cell's membrane [4].

Fig.2: Modified LE-FDTD cell on normal FDTD cell grid [4].

Fig.3: Field distribution in and around a single isolated cell.

Fig.4: Electric Field ( $E_x$ ) distribution along principal axes of a double-layer sphere in lossy medium, excited by a plane wave of 1V/m at 2450GHz.

Fig.5: Electric Field ( $E_z$ ) distribution along the x-axis for double-layer sphere in lossy medium, excited by plane wave of 1V/m at 2450GHz.

Fig.6: Two-dimensional view of the simulated periodic structure in the FDTD computational domain, extended by the Floquet boundary condition.

Fig.7: Three-dimensional view of the basic simulated spherical structures in the FDTD computational domain.

Fig.8: Electric field distribution along z-axis, through the centre of the simulated structure, showing effect of different spacings to the Floquet boundary condition (Ncell is the number of *FDTD* cells from the *biological* cell wall to the boundary).

Fig.9: Electric field distribution (Enlargement of Fig.8)

Fig. 10: Modulus of the electric field on the  $xz$ -plane at intermediate frequency 10GHz, with Floquet boundary spaced 20 FDTD cells from the biological cell walls.

Fig.11: Modulus of the electric field on  $xz$ -plane at intermediate frequency 10GHz, with Floquet boundary adjacent to the biological cell walls.

Fig.12: Electric field distribution along  $z$  axis, through the centre of the simulated structure in Fig. 11.

Fig.13: Electric field distribution along  $z$  axis, through the centre of the simulated structure in Fig. 11 (Enlargement)

Fig.14: Electric field distribution along  $z$ -axis, through the centre of the simulated spherical structure in Fig 11, incorporating HH model and driven at 900MHz.

Fig.15: As Fig. 14, driven at 2450MHz.

Fig.16: Three-dimensional view of the simulated cubical structures in the FDTD computational domain.

Fig.17: Modulus of the electric field on  $xz$ -plane at intermediate frequency 10GHz with Floquet boundary adjacent to the biological cell walls.

Fig.18: Electric field distribution along  $z$ -axis, through the centre of the simulated cubical structure

Fig.19: Electric field distribution along  $z$ -axis, through the centre of the simulated cubical structure (Enlargement of Fig.18)

Fig.20: Electric field distribution along  $z$ -axis, through the centre of the simulated spherical structure in Fig. 17, incorporating HH model and driven at 900MHz.

Fig.21: As Fig. 20, driven at 2450MHz.

Table 1. Electrical properties of the simulated media at relevant frequencies

	900 MHz	1800MHz	2000MHz	2450MHz	10GHz
$\sigma_i$	72.2003	71.956	71.88	71.6806	63.5023
$\varepsilon_i$	0.4168	0.7656	0.8742	1.1590	12.8384
$\varepsilon_m$	1.6526	1.5680	1.5621	1.5536	1.5371
$\sigma_m$	0.0217	0.0232	0.0233	0.0234	0.0237
$\varepsilon_e$	72.2003	71.956	71.88	71.6806	63.5023
$\sigma_e$	1.3168	1.6656	1.7742	2.0590	13.7384

Where subscripts  $i$ ,  $m$ ,  $e$  represent cytoplasm, membrane and extracellular medium respectively.

Table 2. Frequency scaling transformation factor from 10GHz to the mobile communication frequencies given

Parameter	900MHz	1800MHz	2000MHz	2450MHz
Cytoplasm	0.9296	0.9337	0.9344	0.9360
Membrane	0.9	0.97	0.9756	0.9838
Extracellular medium	0.8867	0.9226	0.9254	0.9301

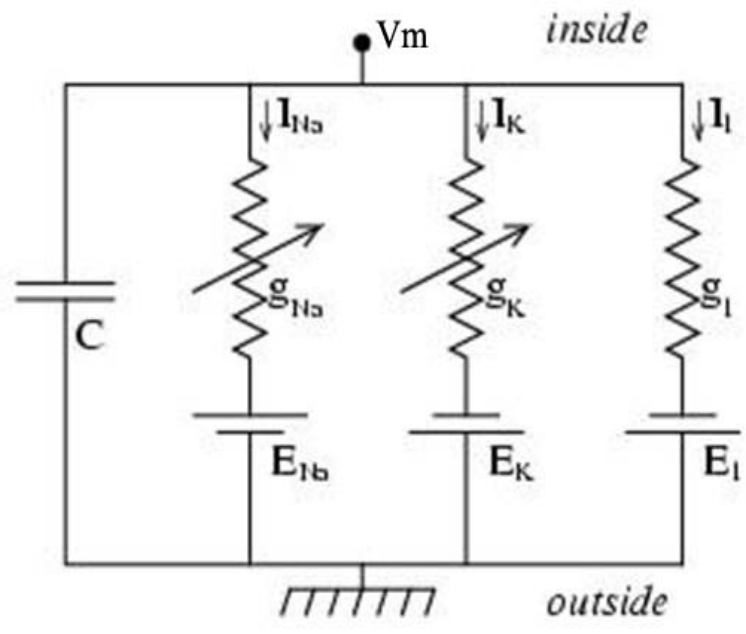


Fig.1: Equivalent electrical circuit for the cell's membrane [4].

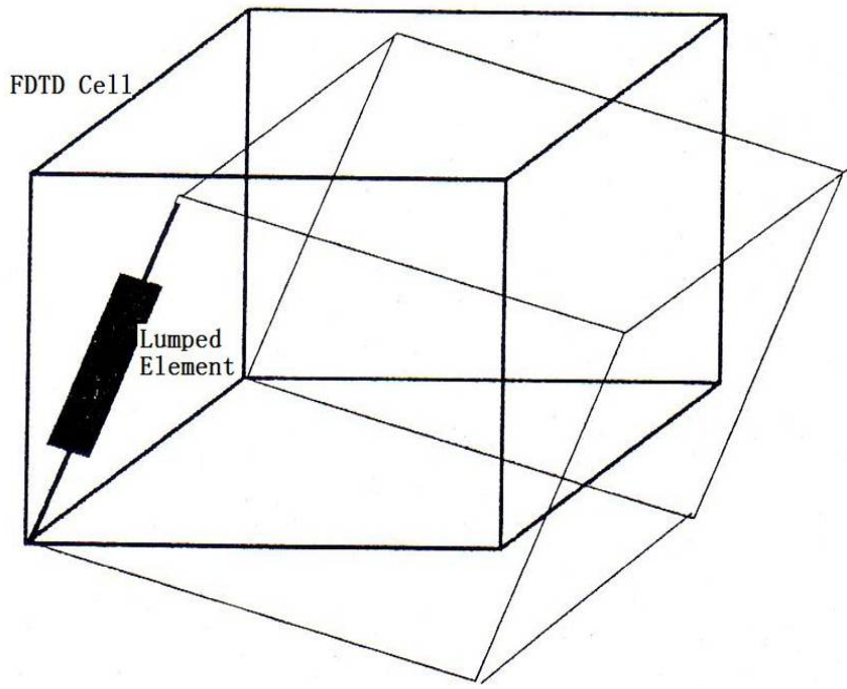


Fig.2: Modified LE-FDTD cell on normal FDTD cell grid [4].

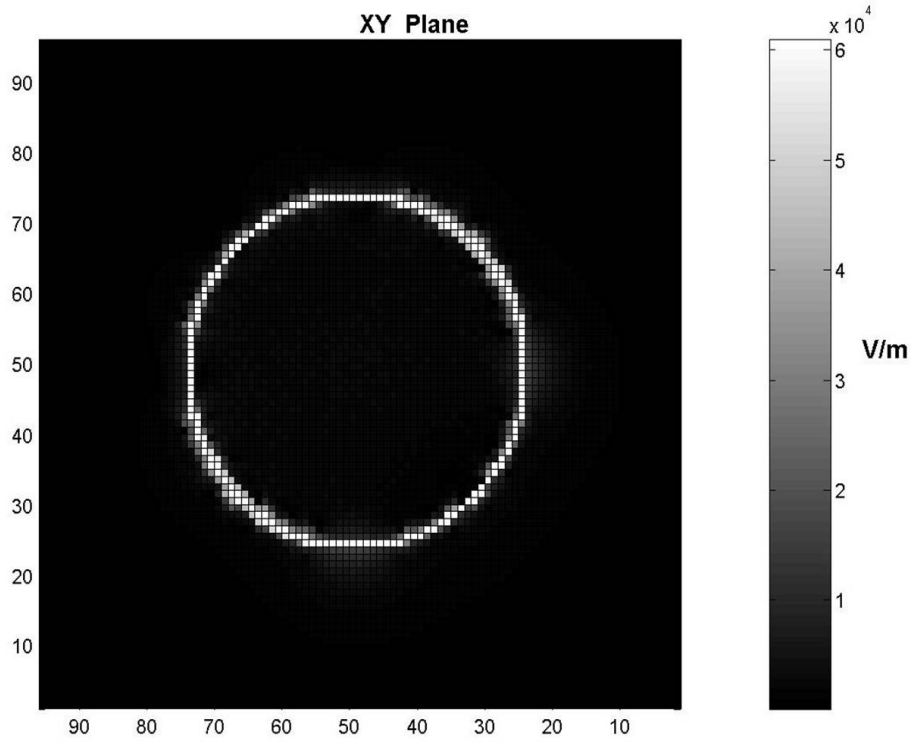


Fig.3: Field distribution in and around a single isolated cell.

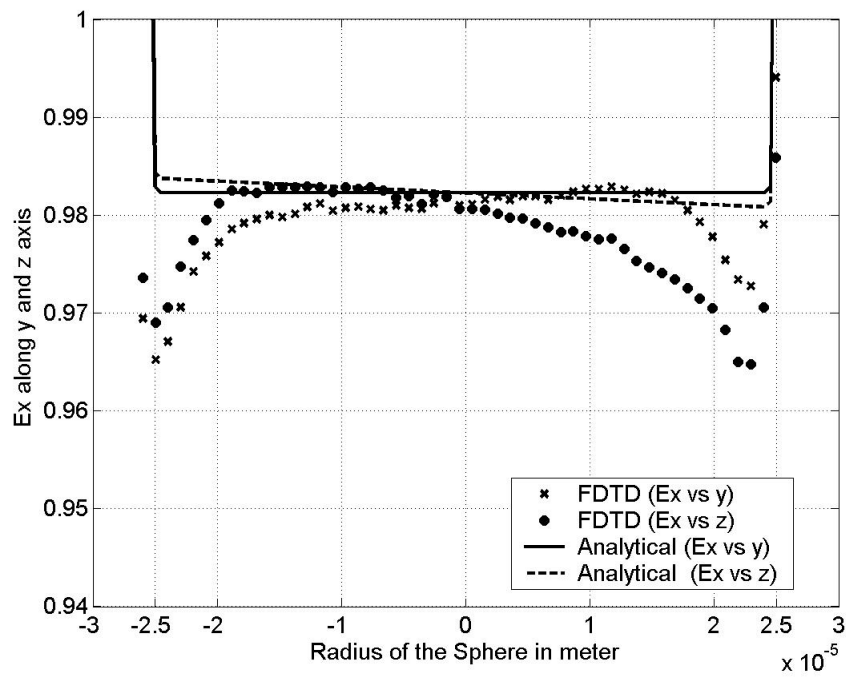


Fig.4: Electric Field ( $E_x$ ) distribution along principal axes of a double-layer sphere in lossy medium, excited by a plane wave of 1V/m at 2450GHz.

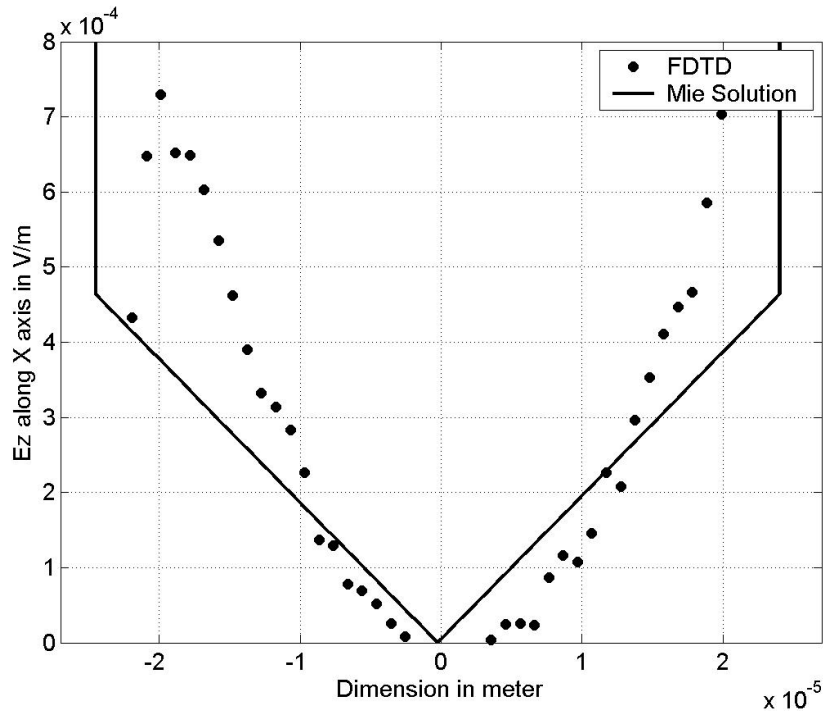


Fig.5: Electric Field ( $E_z$ ) distribution along the x-axis for double-layer sphere in lossy medium, excited by plane wave of 1V/m at 2450GHz.

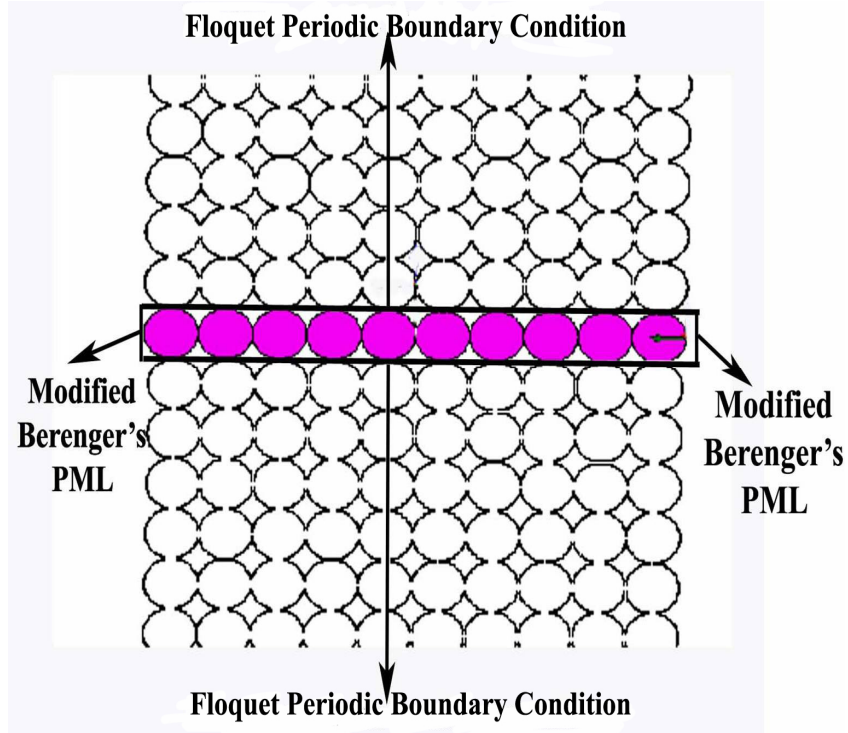


Fig.6: Two-dimensional view of the simulated periodic structure in the FDTD computational domain, extended by the Floquet boundary condition.

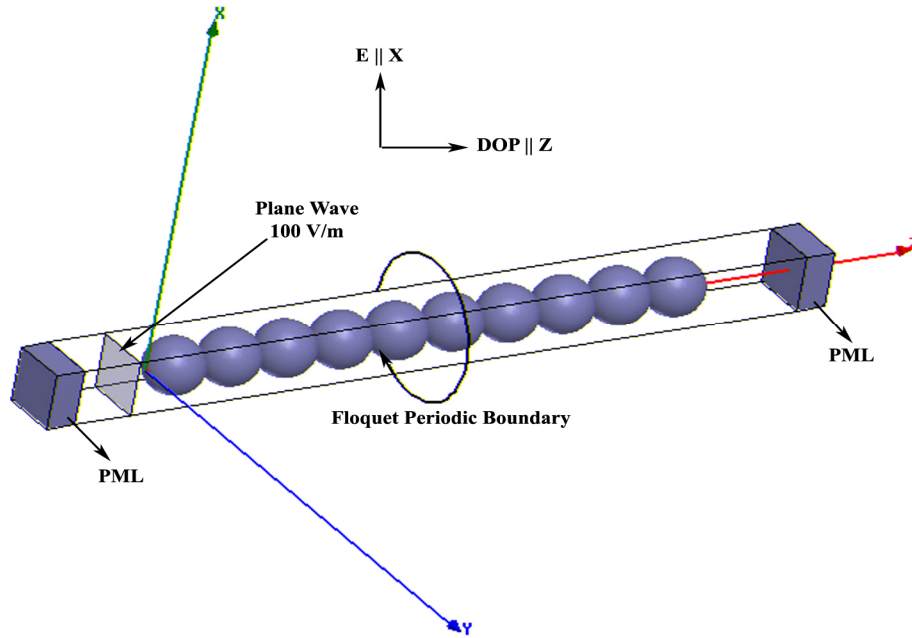


Fig.7: Three-dimensional view of the basic simulated spherical structures in the FDTD computational domain.

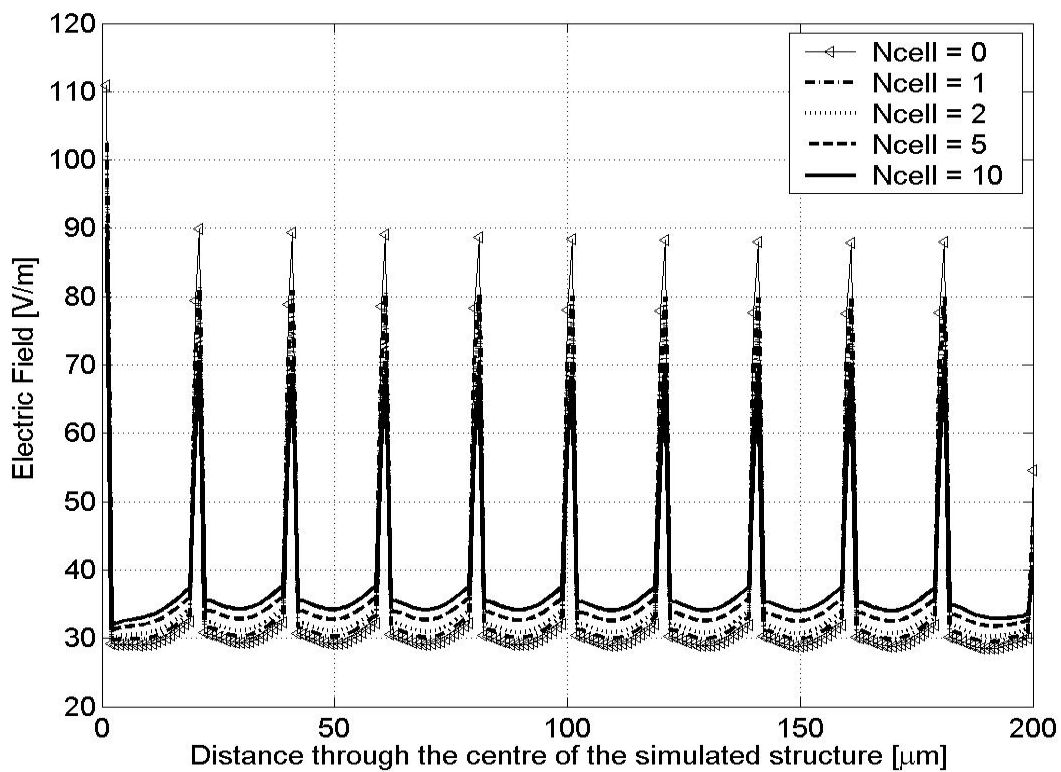


Fig.8: Electric field distribution along z-axis, through the centre of the simulated structure, showing effect of different spacings to the Floquet boundary condition (Ncell is the number of *FDTD* cells from the *biological* cell wall to the boundary).



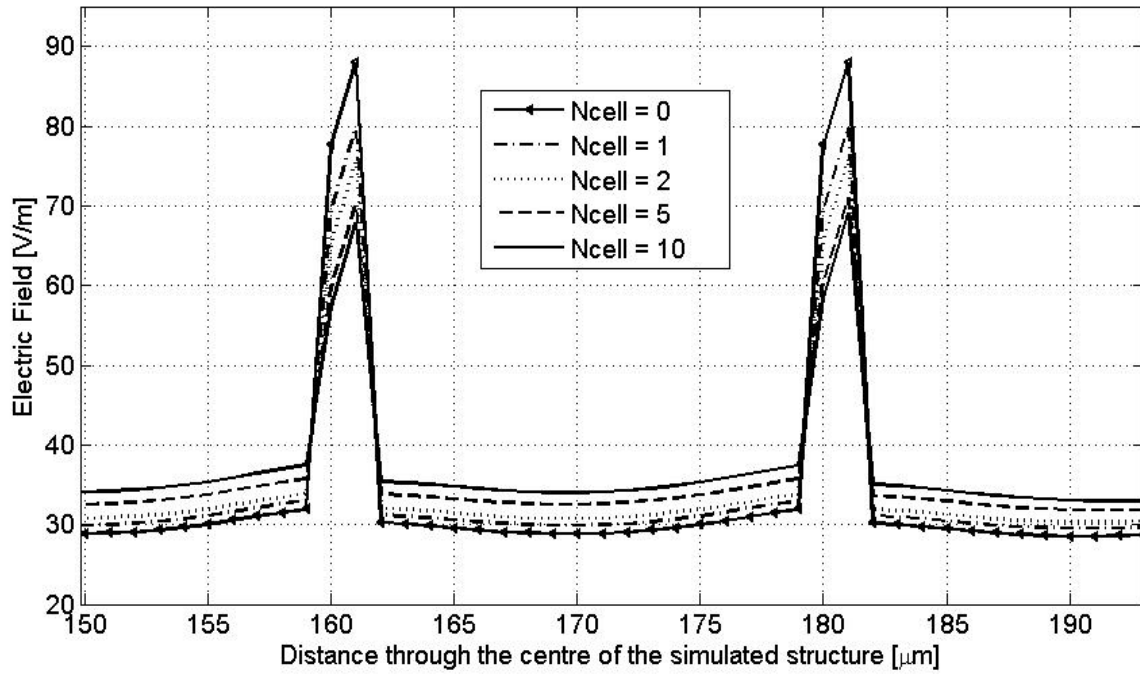


Fig.9: Electric field distribution (Enlargement of Fig.8)

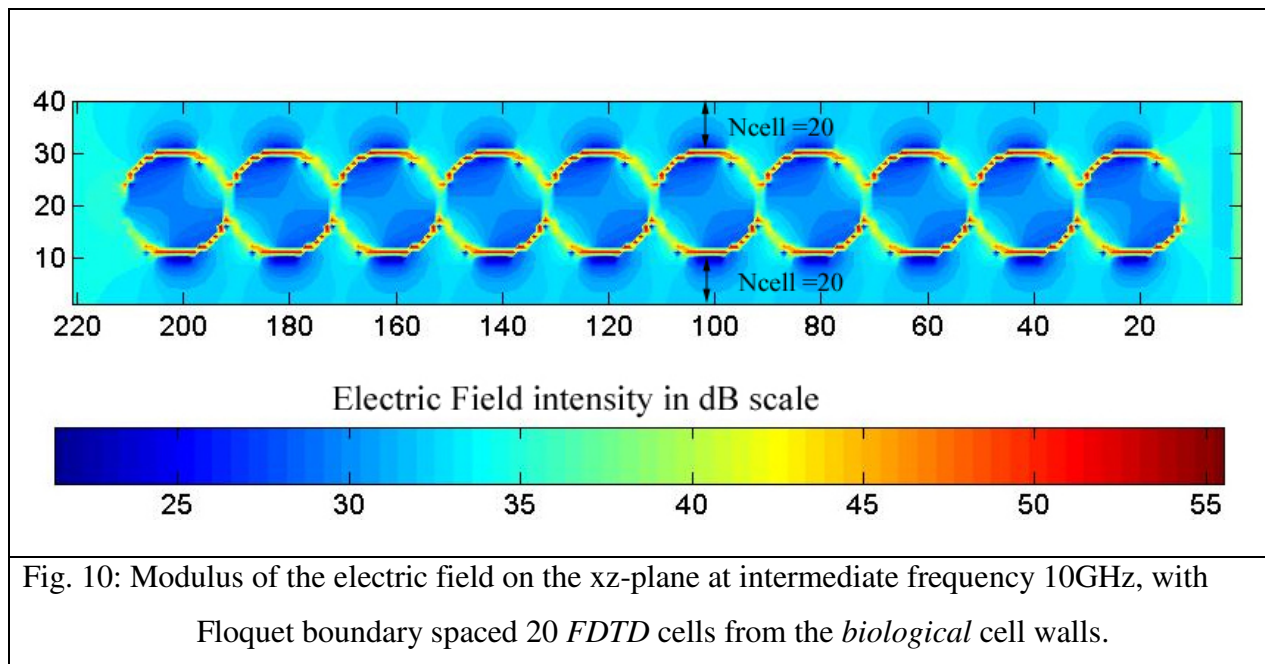


Fig. 10: Modulus of the electric field on the  $xz$ -plane at intermediate frequency 10GHz, with Floquet boundary spaced 20 *FDTD* cells from the *biological* cell walls.

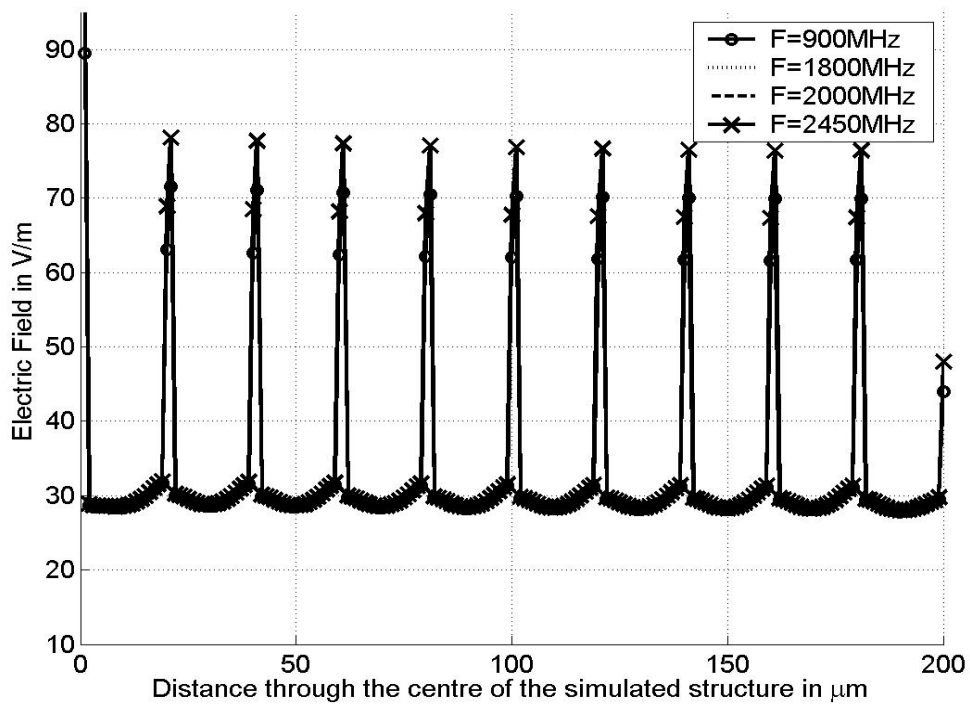
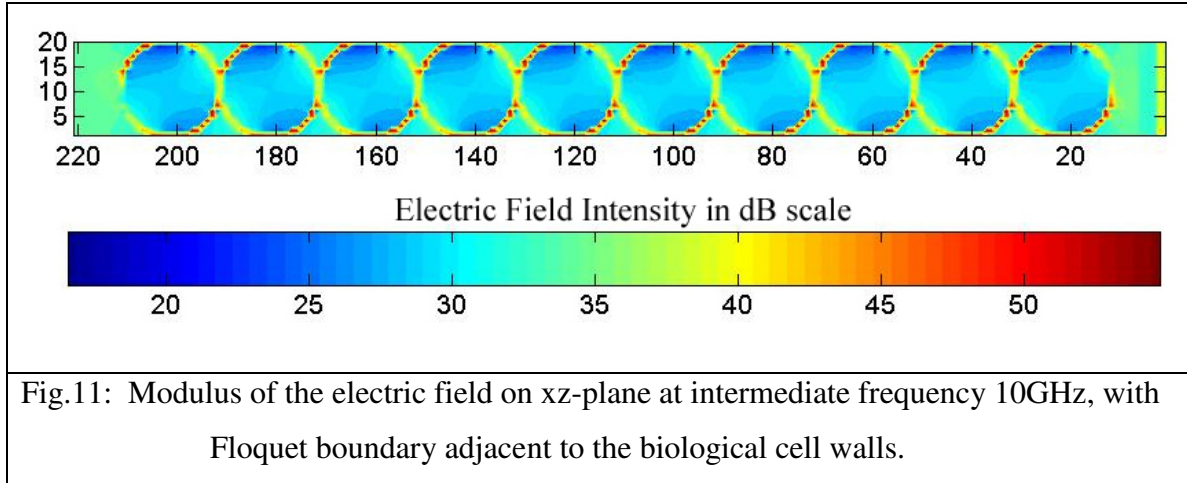


Fig.12: Electric field distribution along z axis, through the centre of the simulated structure in Fig. 11.

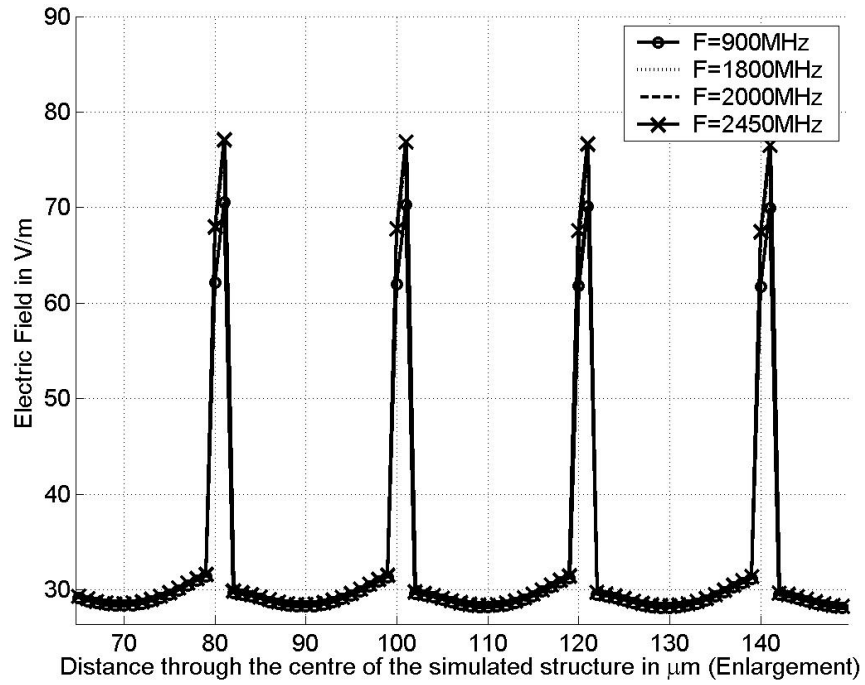


Fig.13: Electric field distribution along z axis, through the centre of the simulated structure in Fig. 11 (Enlargement)

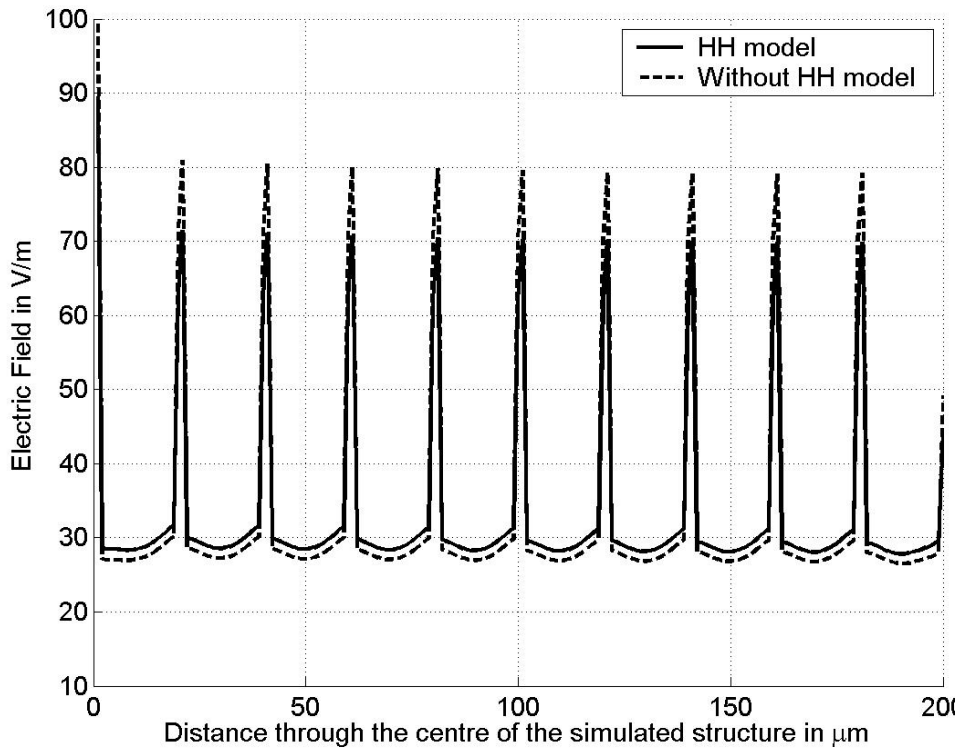


Fig.14: Electric field distribution along z-axis, through the centre of the simulated spherical structure in Fig 11, incorporating HH model and driven at 900MHz.

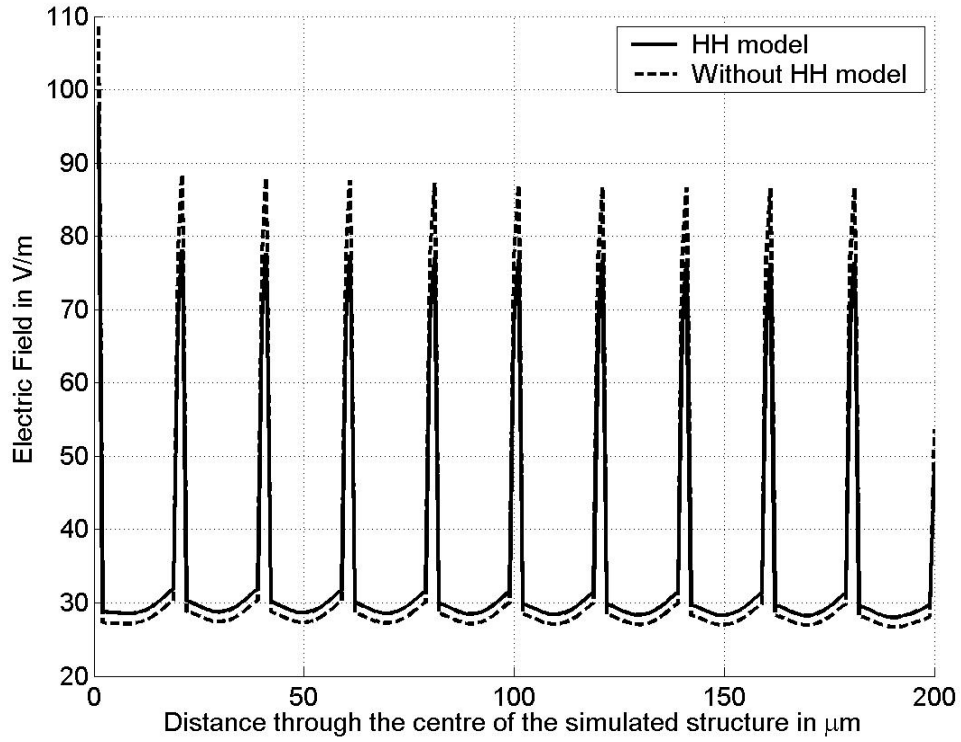


Fig.15: As Fig. 14, driven at 2450MHz.

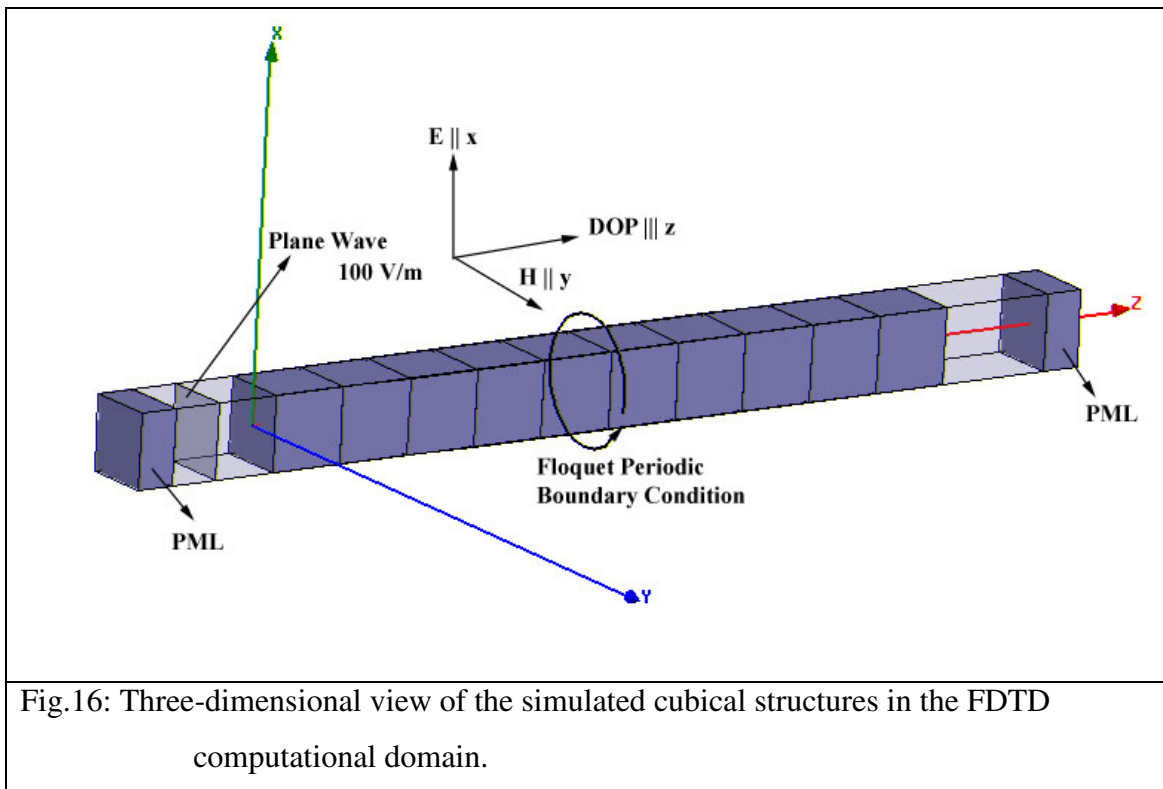


Fig.16: Three-dimensional view of the simulated cubical structures in the FDTD computational domain.

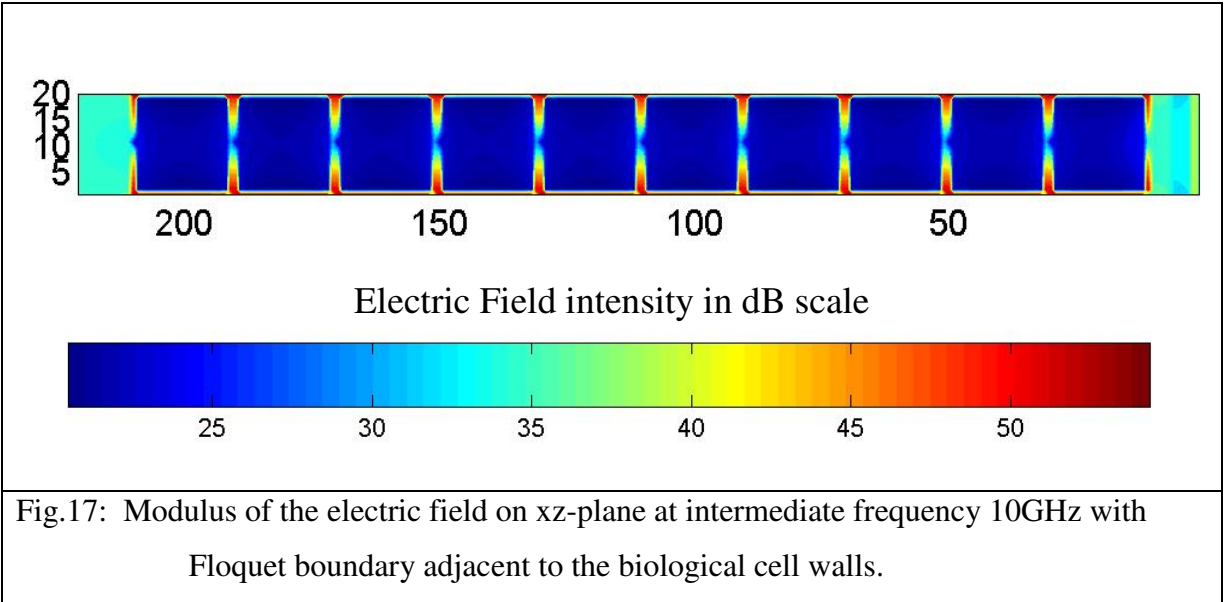


Fig.17: Modulus of the electric field on xz-plane at intermediate frequency 10GHz with Floquet boundary adjacent to the biological cell walls.

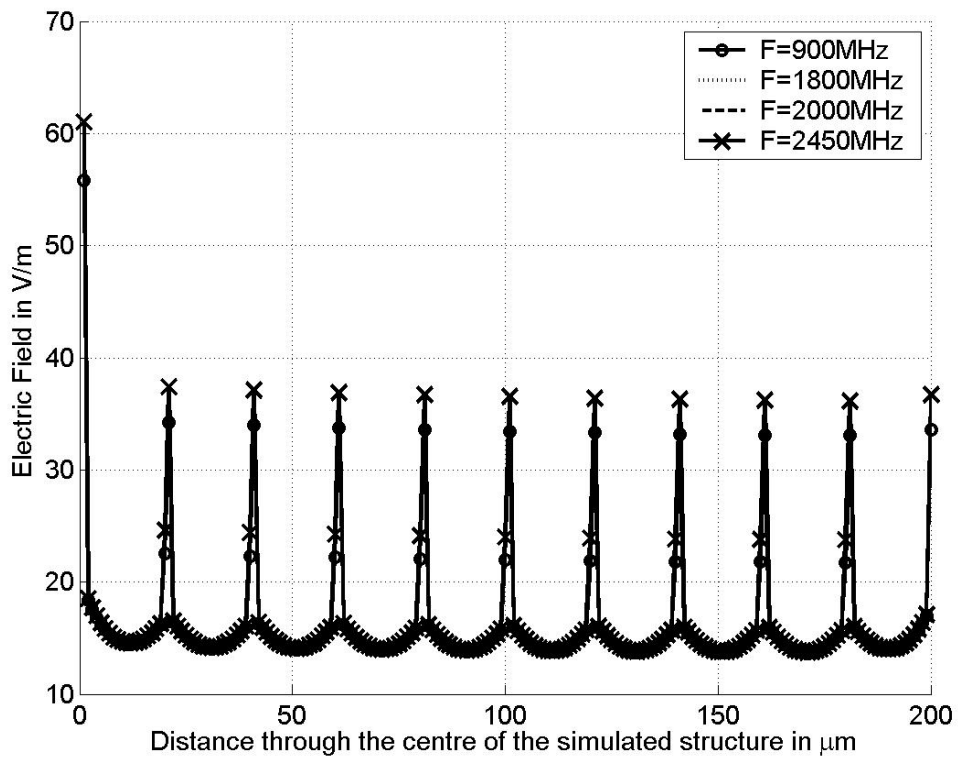


Fig.18: Electric field distribution along z-axis, through the centre of the simulated cubical structure

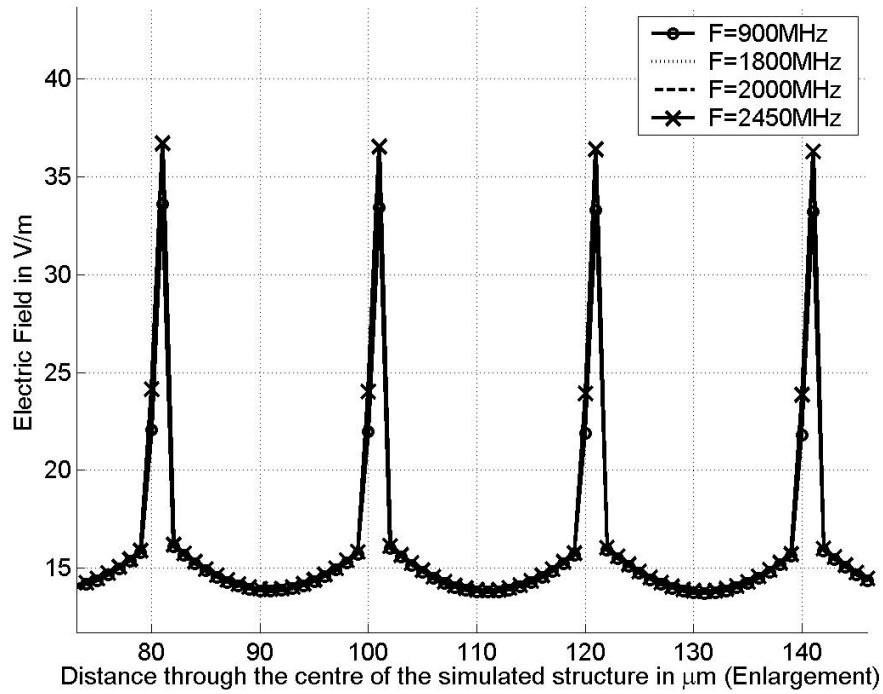


Fig.19: Electric field distribution along z-axis, through the centre of the simulated cubical structure (Enlargement of Fig.18)

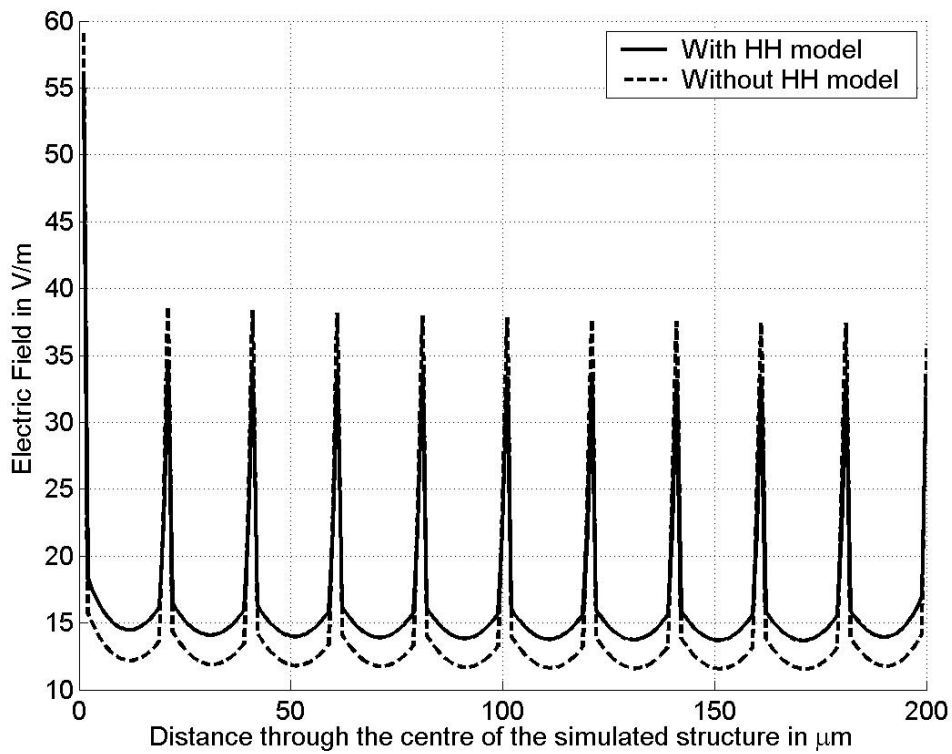


Fig.20: Electric field distribution along z-axis, through the centre of the simulated spherical structure in Fig. 17, incorporating HH model and driven at 900MHz.

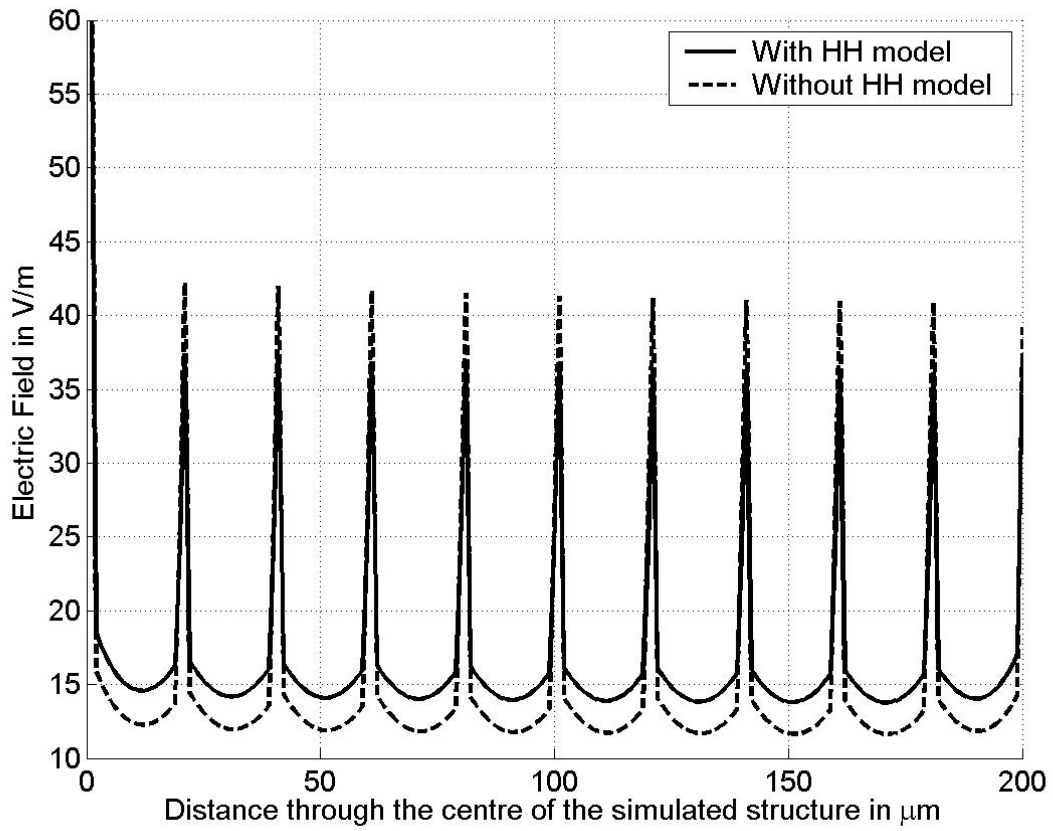


Fig.21: As Fig. 20, driven at 2450MHz.